

# Algorithmic Design of Majorizers for Large-Scale Inverse Problems

Madison G. McGaffin

Jeffrey A. Fessler

Department of Electrical Engineering and Computer Science  
University of Michigan, Ann Arbor, MI

April 10, 2024

## Abstract

Iterative majorize-minimize (MM) (also called optimization transfer) algorithms solve challenging numerical optimization problems by solving a series of “easier” optimization problems that are constructed to guarantee monotonic descent of the cost function. Many MM algorithms replace a computationally expensive Hessian matrix with another more computationally convenient majorizing matrix. These majorizing matrices are often generated using various matrix inequalities, and consequently the set of available majorizers is limited to structures for which these matrix inequalities can be efficiently applied. In this paper, we present a technique to algorithmically design matrix majorizers with wide varieties of structures. We use a novel duality-based approach to avoid the high computational and memory costs of standard semidefinite programming techniques. We present some preliminary results for 2D X-ray CT reconstruction that indicate these more exotic regularizers may significantly accelerate MM algorithms.

## I. INTRODUCTION

Given an  $N \times N$  Hermitian matrix  $\mathbf{H}$ , we say that the Hermitian matrix  $\mathbf{M}$  majorizes  $\mathbf{H}$  if none of the eigenvalues of  $\mathbf{M} - \mathbf{H}$  are negative. Matrix majorizers are central to majorize-minimize algorithms and are ubiquitous in image processing algorithms [1], [4], [15], [21]. Better majorizers can significantly affect how quickly algorithms converge [6], [11], [15], but majorizers are usually designed by hand on a per-problem basis. Algorithmic majorizer design expands the class of usable majorizers and reveals more effective majorizers, but a straightforward semidefinite programming approach requires too much memory to be computationally feasible for many practical imaging problems.

This paper presents an algorithmic approach to designing a majorizing matrix  $\mathbf{M}$  for a general given Hermitian  $\mathbf{H}$ . The algorithm we present has relatively low memory requirements, and it is practical for large problems where storing and manipulating dense  $N \times N$  matrices would be infeasible. The goal of this chapter is to enable the design of more exotic majorizers than are currently accessible using various inequalities. This expanded class of majorizers may contain tighter majorizers [6] that lead to faster convergence [7].

Conventionally, a majorizing matrix  $\mathbf{M} \succeq \mathbf{H}$  is found using a collection of inequalities and matrix properties. A simple and common bound is  $\mathbf{M}_{\text{Lipschitz}} = \lambda_{\max}(\mathbf{H})\mathbf{I}$ , which is often used in optimization algorithms for which the cost function gradient is Lipschitz continuous (with Lipschitz constant  $\lambda_{\max}(\mathbf{H})$ ). This choice often is a very loose bound. Often a tighter bound is the diagonal matrix

$$\mathbf{M}_{\text{SQS}} = \text{diag} \left\{ \sum_{i=1}^N |\mathbf{H}|_{ij} \right\}. \quad (1)$$

We call this the “separable quadratic surrogates” (SQS) majorizer due to its ubiquity in ordered subsets with SQS (OS-SQS) algorithms [1]. If  $\mathbf{H}$  contains only nonnegative entries (e.g.,  $\mathbf{A}^T \mathbf{W} \mathbf{A}$ , the Hessian of the X-ray CT data-fit term [1], [23]) then  $\mathbf{M}_{\text{SQS}}$  can be quickly computed via

$$\mathbf{M}_{\text{SQS}} = \text{diag} \left\{ [\mathbf{H}\mathbf{1}]_j \right\}. \quad (2)$$

Our experiments (not shown) suggest that  $\mathbf{M}_{\text{SQS}}$  is a fairly tight diagonal majorizer when  $\mathbf{H}$  contains only nonnegative entries, and its ease of computation (2) makes it a very useful tool. However, when  $\mathbf{H}$  contains negative entries,  $\mathbf{M}_{\text{SQS}}$  appears to be less tight. In this case, carefully designed majorizers that exploit the structure of  $\mathbf{H}$ , e.g., [15], can significantly improve on  $\mathbf{M}_{\text{SQS}}$ .

This paper focuses on designing majorizers of the following form:

$$\mathbf{M} = \mathbf{K}^H \mathbf{D} \mathbf{K}, \quad (3)$$

where  $\mathbf{D} \in \mathbb{R}^{K \times K}$  is a diagonal matrix and  $\mathbf{K} \in \mathbb{C}^{K \times N}$ ,  $K \geq N$  has full column rank. We assume the matrix  $\mathbf{K}$  is selected by the MM algorithm designer beforehand and focus on designing  $\mathbf{D}$ . A special case is  $\mathbf{K} = \mathbf{I}$ , which leads to a diagonal

majorizer. Our goal is to select the diagonal matrix  $\mathbf{D}$  such that  $\mathbf{M}$  is a majorizer of  $\mathbf{H}$  and such that the values of  $\mathbf{D}$  are “as small as possible” so that the majorizer is “tight” or “sharp.” To quantify this goal, we pose the following convex optimization problem:

$$\mathbf{M} = \mathbf{K}^\top \hat{\mathbf{D}} \mathbf{K}, \quad \text{where} \quad (4)$$

$$\hat{\mathbf{D}} = \underset{\mathbf{D}: \mathbf{K}^\top \mathbf{D} \mathbf{K} \succeq \mathbf{H}}{\operatorname{argmin}} \frac{1}{2} \|\mathbf{d}\|_{\mathbf{W}}^2, \quad (5)$$

with positive diagonal weighting matrix  $\mathbf{W}$ . The vector  $\mathbf{d} \in \mathbb{R}^N$  is the diagonal  $\mathbf{D}$ .

## II. METHODS

Let  $\mathbf{H} \in \mathbb{C}^{N \times N}$  be a given Hermitian positive semidefinite matrix, and let  $\mathbf{K} \in \mathbb{C}^{K \times N}$  be a given matrix with full column rank. We aim to majorize  $\mathbf{H}$  with the matrix  $\mathbf{K}^\top \hat{\mathbf{D}} \mathbf{K}$ , where  $\hat{\mathbf{D}}$  solves

$$\hat{\mathbf{D}} = \underset{\mathbf{D}: \mathbf{K}^\top \mathbf{D} \mathbf{K} \succeq \mathbf{H}}{\operatorname{argmin}} \frac{1}{2} \|\mathbf{d}\|_{\mathbf{W}}^2. \quad (6)$$

The vector  $\mathbf{d} \in \mathbb{R}^K$  is the diagonal of  $\mathbf{D}$ , and  $\mathbf{W} \in \mathbb{R}^{K \times K}$  is a given positive-definite weighting matrix. This is a convex minimization problem over a convex set, although the domain  $\Omega$ ,

$$\Omega = \{\mathbf{d} : \mathbf{K}^\top \mathbf{D} \mathbf{K} \succeq \mathbf{H}\} \quad (7)$$

is challenging to efficiently characterize. The majorizer design problem we pose (6) could be solved using a semidefinite programming (SDP) technique. However, to the best of our knowledge, algorithms to solve (6) using SDP involve storing and manipulating dense  $N \times N$  matrices [2], [8]. In practical image processing problems,  $N$  is the number of pixels in the image and can be very large, so storing arbitrary  $N \times N$  matrices is infeasible.

We rewrite the majorizer design problem (6) using the characteristic function  $\iota_\Omega$  as

$$\hat{\mathbf{D}} = \underset{\mathbf{d} \in \mathbb{R}^K}{\operatorname{argmin}} \frac{1}{2} \|\mathbf{d}\|_{\mathbf{W}}^2 + \iota_\Omega(\mathbf{d}). \quad (8)$$

The characteristic function  $\iota_\Omega(\mathbf{d})$  is zero when  $\mathbf{d} \in \Omega$  (i.e.,  $\mathbf{K}^\top \mathbf{D} \mathbf{K}$  majorizes  $\mathbf{H}$ ) and infinite otherwise. Instead of directly approaching (8), we rewrite the characteristic function  $\iota_\Omega$  using a generalized convex conjugate [19]:

$$\iota_\Omega(\mathbf{d}) = \sup_{\mathbf{z} \in \mathbb{C}^N} \mathbf{z}^\top (\mathbf{H} - \mathbf{K}^\top \mathbf{D} \mathbf{K}) \mathbf{z} \quad (9)$$

$$= \sup_{\mathbf{z} \in \mathbb{C}^N} \mathbf{z}^\top \mathbf{H} \mathbf{z} - (\mathbf{K} \mathbf{z})^\top \mathbf{D} (\mathbf{K} \mathbf{z}) \quad (10)$$

$$= \sup_{\mathbf{z} \in \mathbb{C}^N} \mathbf{z}^\top \mathbf{H} \mathbf{z} - \mathbf{d}^\top |\mathbf{K} \mathbf{z}|^2, \quad (11)$$

where  $|\mathbf{K} \mathbf{z}|^2$  contains the elementwise squared complex moduli of  $\mathbf{K} \mathbf{z}$ :

$$|\mathbf{K} \mathbf{z}|^2 = \operatorname{vec} \left\{ |\mathbf{K} \mathbf{z}|_k^2 \right\}. \quad (12)$$

Substituting (11) in (8) yields the following min-max problem for designing  $\mathbf{D}$ :

$$\hat{\mathbf{D}} = \underset{\mathbf{d} \in \mathbb{R}^K}{\operatorname{argmin}} \sup_{\mathbf{z} \in \mathbb{C}^N} S(\mathbf{d}, \mathbf{z}), \quad (13)$$

$$S(\mathbf{d}, \mathbf{z}) = \frac{1}{2} \|\mathbf{d}\|_{\mathbf{W}}^2 - \mathbf{d}^\top |\mathbf{K} \mathbf{z}|^2 + \mathbf{z}^\top \mathbf{H} \mathbf{z}. \quad (14)$$

Reversing the order of the “argmin” and “sup” in (13) and solving for the minimizing  $\mathbf{d}$  in terms of  $\mathbf{z}$  yields the dual problem

$$\hat{\mathbf{z}} = \underset{\mathbf{z} \in \mathbb{C}^N}{\operatorname{argmax}} L(\mathbf{z}), \quad \text{where} \quad (15)$$

$$L(\mathbf{z}) = -\frac{1}{2} \left\| |\mathbf{K} \mathbf{z}|^2 \right\|_{\mathbf{W}^{-1}}^2 + \mathbf{z}^\top \mathbf{H} \mathbf{z}. \quad (16)$$

We solve this dual problem to recover the the optimal primal variable  $\hat{\mathbf{D}}$ . This requires the following two results:

- Strong duality, i.e.,

$$\inf_{\mathbf{d} \in \mathbb{R}^K} \sup_{\mathbf{z} \in \mathbb{C}^N} S(\mathbf{d}, \mathbf{z}) = \sup_{\mathbf{z} \in \mathbb{C}^N} \inf_{\mathbf{d} \in \mathbb{R}^K} S(\mathbf{d}, \mathbf{z}). \quad (17)$$

Appendix A provides a proof.

- A way to recover the primal variable  $\hat{\mathbf{D}}$  from a dual solution  $\hat{\mathbf{z}}$ . Appendix B shows

$$\hat{\mathbf{d}} = \mathbf{W}^{-1} |\mathbf{K}\hat{\mathbf{z}}|^2, \quad (18)$$

where  $\hat{\mathbf{z}}$  solves the dual problem.

We have found a dual problem for the majorizer design problem (6). Unlike the original problem, the dual problem does not directly use the difficult-to-characterize domain  $\Omega$  and can be approached without memory- and computationally-expensive SDP techniques. The drawback of this transformation is that the dual problem (15) is not concave. Consequently, the steepest ascent algorithm in Section II-A may converge to a local optimum. Nonetheless these suboptimal solutions may be useful, and Section II-B discusses modifications of these local optima to provide a matrix that majorizes  $\mathbf{H}$ .

#### A. Dual steepest ascent

We find a local maximizer of the dual function  $L$  using steepest ascent. Initialize  $\hat{\mathbf{z}}^{(0)} \neq \mathbf{0}$ . We compute the search  $\mathbf{g}^{(n)}$  direction using the gradient of  $L(\mathbf{z}^{(n)})$ :

$$\mathbf{g}^{(n)} = \nabla L(\mathbf{z}^{(n)}) \quad (19)$$

$$= 2(\mathbf{H}\mathbf{z} - \mathbf{K}^H \mathbf{W}^{-1} |\mathbf{K}\mathbf{z}|^2 \odot \mathbf{K}\mathbf{z}), \quad (20)$$

where  $\odot$  is element-wise multiplication. Maximizing the dual function  $L$  along this search direction involves solving the following line search problem:

$$\alpha^{(n)} = \underset{\alpha \in \mathbb{R}}{\operatorname{argmax}} f^{(n)}(\alpha), \quad \text{where} \quad (21)$$

$$f^{(n)}(\alpha) = L(\mathbf{z}^{(n)} + \alpha \mathbf{g}^{(n)}). \quad (22)$$

Setting  $(f^{(n)})'(\alpha) = 0$  yields

$$0 = c_3 \alpha^3 + c_2 \alpha^2 + c_1 \alpha + c_0, \quad \text{where} \quad (23)$$

$$c_3 = 2\mathbf{v}_2^T \mathbf{W}^{-1} \mathbf{v}_2 \quad (24)$$

$$c_2 = 3\mathbf{v}_2^T \mathbf{W}^{-1} \mathbf{v}_1 \quad (25)$$

$$c_1 = 2\mathbf{v}_2^T \mathbf{W}^{-1} \mathbf{v}_0 + \mathbf{v}_1^T \mathbf{W}^{-1} \mathbf{v}_1 - 2b_2 \quad (26)$$

$$c_0 = \mathbf{v}_1^T \mathbf{W}^{-1} \mathbf{v}_0 - b_1, \quad (27)$$

$$\mathbf{v}_2 = |\mathbf{K}\mathbf{g}^{(n)}|^2 \quad \mathbf{b}_2 = (\mathbf{g}^{(n)})^H \mathbf{H}\mathbf{g}^{(n)} \quad (28)$$

$$\mathbf{v}_1 = 2 \cdot \operatorname{Real}\{\mathbf{K}\mathbf{g}^{(n)} \odot \mathbf{K}\mathbf{z}^{(n)}\} \quad \mathbf{b}_1 = 2 \cdot \operatorname{Real}\left\{(\mathbf{g}^{(n)})^H \mathbf{H}\mathbf{z}^{(n)}\right\} \quad (29)$$

$$\mathbf{v}_0 = |\mathbf{K}\mathbf{z}^{(n)}|^2. \quad (30)$$

The root-finding problem (23) can be solved using an off-the-shelf routine, e.g., `roots` in the software package `octave`. We loop over the real roots of  $(f^{(n)})'(\alpha)$  and choose the step length  $\alpha^{(n)}$  that maximizes the dual function.

Each iteration of the proposed algorithm requires one multiplication by  $\mathbf{H}$  and one multiplication by  $\mathbf{K}$  and  $\mathbf{K}^H$ , and the algorithm stores only length- $N$  and  $-K$  vectors. Thus the algorithm is practical even for large-scale problems like CT image reconstruction where one must compute  $\mathbf{H}\mathbf{z}$  on the fly. This procedure will find a local maximizer of the dual function; the next section discusses how to manipulate the resulting approximate solution to produce a majorizer of  $\mathbf{H}$ .

#### B. Ensuring majorization

The dual problem (15) is not concave, so the steepest ascent algorithm in this section will not in general converge to a global maximizer of the dual function  $L$ . This means that the induced matrix,

$$\mathbf{K}^H \tilde{\mathbf{D}} \mathbf{K} = \mathbf{K}^H \mathbf{W}^{-1} \operatorname{diag} \left\{ \left[ |\mathbf{K}\hat{\mathbf{z}}|^2 \right]_i \right\} \mathbf{K}, \quad (31)$$

may not majorize  $\mathbf{H}$ . To compensate for this possible suboptimality, we scale the resulting matrix:

$$\tilde{\mathbf{M}} = \alpha \mathbf{K}^T \tilde{\mathbf{D}} \mathbf{K} \succeq \mathbf{H}, \quad \text{where} \quad (32)$$

$$\alpha \in \left[ \lambda_{\max} \left( \left( \mathbf{K}^H \tilde{\mathbf{D}} \mathbf{K} \right)^{-\frac{1}{2}} \mathbf{H} \left( \mathbf{K}^H \tilde{\mathbf{D}} \mathbf{K} \right)^{-\frac{1}{2}} \right), 3 \right]. \quad (33)$$

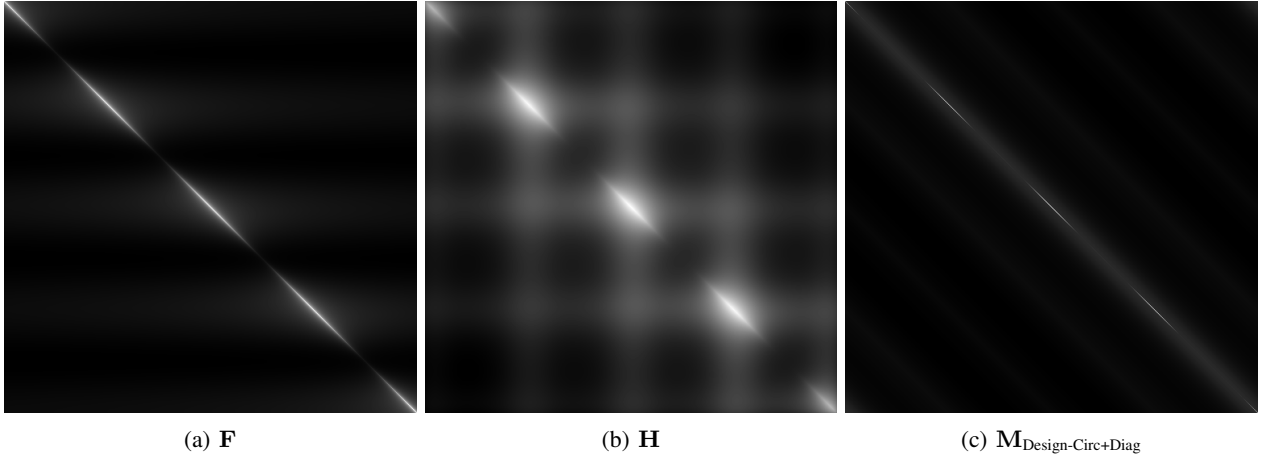


Fig. 1: The nonnegative matrices  $\mathbf{F}$  and  $\mathbf{H}$  from the experiment in Section III-A, and the matrix  $\mathbf{M}_{\text{Design-Circ+Diag}}$  produced by our proposed algorithm.

This results in a majorizer for  $\mathbf{H}$ ; see Appendix C for a proof. If  $(\mathbf{K}^H \tilde{\mathbf{D}} \mathbf{K})^{-\frac{1}{2}}$  is easily computed, then power iteration can be used to find the optimal (minimal) of  $\alpha$ . This will be the case when e.g.,  $\mathbf{K}$  is a unitary matrix. If  $\mathbf{K}$  is more complicated, power iteration may be undesirably computationally expensive, and we instead use the looser scaling  $\alpha = 3$ .

### III. PRELIMINARY EXPERIMENTS

#### A. Weighted Toeplitz matrices and circulant majorizers

We generated the  $N \times N$  weighted Toeplitz matrix  $\mathbf{F}$  with  $N = 512$  and entries

$$[\mathbf{F}]_{ij} = \frac{0.1 + \cos^2(2\pi \frac{i}{N})}{\sqrt{1 + |i - j|}} \quad (34)$$

and set  $\mathbf{H} = \mathbf{F}^T \mathbf{F}$ . This choice is inspired by the  $1/r$ -like response of the CT system matrix [5]. Figures 1a and 1b show  $\mathbf{F}$  and  $\mathbf{H}$ , respectively. We generated three diagonal majorizers:

- $\mathbf{M}_{\text{Lipschitz}} = \lambda_{\max}(\mathbf{H})\mathbf{I}$ ,
- $\mathbf{M}_{\text{SQS}}$  using (2), and
- $\mathbf{M}_{\text{Design-Diag}}$ , using the algorithming proposed in this chapter with  $\mathbf{K} = \mathbf{I}$ .

We also generated  $\mathbf{M}_{\text{Design-Circ+Diag}}$ , a combination of circulant and diagonal matrices, using the proposed algorithm with

$$\mathbf{K}_{\text{Circ+Diag}} = \begin{bmatrix} \mathbf{U}_{\text{DFT}} \\ \mathbf{I} \end{bmatrix}. \quad (35)$$

Finally, we computed  $\mathbf{M}_{\text{Circ}}$

$$\mathbf{M}_{\text{Circ}} = \beta \hat{\mathbf{C}}, \quad (36)$$

where  $\hat{\mathbf{C}}$  is the best circulant approximation to  $\mathbf{F}$  in the Frobenius-norm sense [3],

$$\hat{\mathbf{C}} = \underset{\mathbf{C} \text{ circulant}}{\operatorname{argmin}} \|\mathbf{C} - \mathbf{H}\|_{\mathbf{F}}^2, \quad (37)$$

and  $\beta$  is chosen with power iteration so  $\beta \hat{\mathbf{C}} \succeq \mathbf{H}$ .

We used each of the majorizers to solve the quadratic minimization problem

$$\hat{\mathbf{x}} = \underset{\mathbf{x}}{\operatorname{argmin}} \frac{1}{2} \mathbf{x}^T \mathbf{H} \mathbf{x} + \mathbf{x}^T \mathbf{g}, \quad (38)$$

with  $\mathbf{g}$  and  $\mathbf{x}^{(0)}$  initialized with zero-mean normal random values. We performed the following simple majorize-minimize (MM) procedure:

$$\mathbf{x}^{(n+1)} = \mathbf{x}^{(n)} - \mathbf{M}^{-1}(\mathbf{H} \mathbf{x}^{(n)} + \mathbf{g}). \quad (39)$$

This experiment explores the relative accelerations that different majorizers provide. To solve (38) even faster with a majorize-minimize algorithm, we would also use some first-order acceleration scheme [10], [16], [17]. Figure 2a shows how quickly the MM algorithm iterates  $\{\mathbf{x}^{(n)}\}$  converged to the solution of (38) as a function of iteration with each of the majorizers,

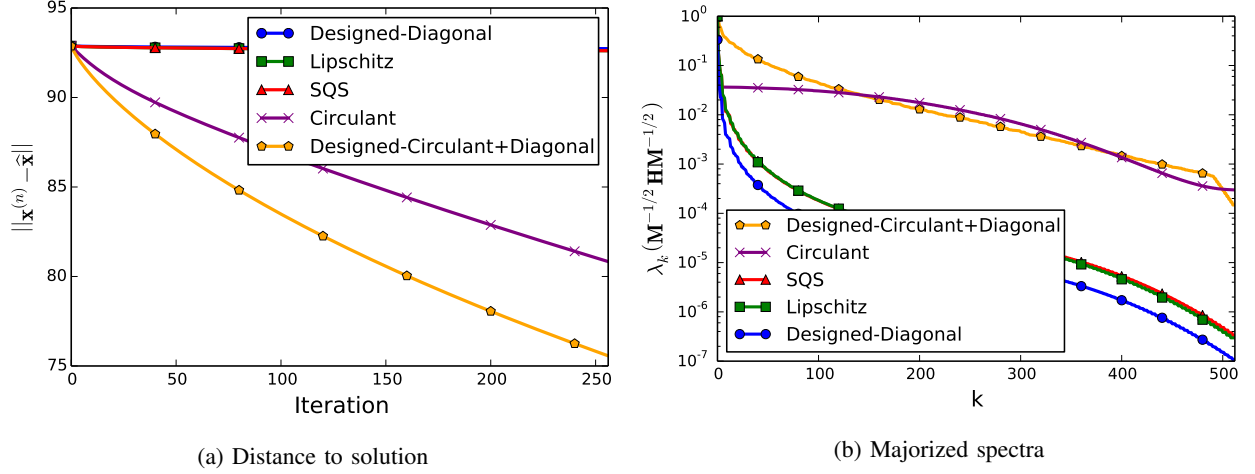


Fig. 2: Convergence plots and majorized spectra for the small Toeplitz experiment in Section III-A. The partially circulant majorizer  $\mathbf{M}_{\text{Design-Circ+Diag}}$  acts like both a majorizer and a preconditioner, accelerating convergence of the simple majorize-minimize algorithm. The ideal majorizer inverts the matrix  $\mathbf{H}$  and produces a uniform majorized spectrum with value 1.

and Figure 2b shows the eigenvalues of  $\mathbf{M}^{-1/2}\mathbf{H}\mathbf{M}^{-1/2}$  for each majorizer  $\mathbf{M}$ . For fast convergence, ideally those eigenvalues would be near 1 [7].

The designed diagonal majorizer underperforms the more conventional SQS majorizer,  $\mathbf{M}_{\text{SQS}}$ . This is possibly due to the proposed algorithm producing a suboptimal solution to the majorizer design dual problem. Regardless, diagonal majorizers are not our primary interest here: the proposed algorithm is more useful for generating majorizers with more exotic structures.

Except for edge conditions, circulant matrices and Toeplitz matrices are very similar. Because  $\mathbf{M}_{\text{Circ}}$  and  $\mathbf{M}_{\text{Design-Circ+Diag}}$  contain circulant terms, they can approximate  $\mathbf{H}$  while majorizing it. When these matrices are inverted in the majorize-minimize procedure (39), they act as both preconditioners and majorizers. The preconditioning effect appears in better-conditioned spectra (i.e., closer to uniform 1s) for  $\mathbf{M}_{\text{Circ}}$  and  $\mathbf{M}_{\text{Design-Circ+Diag}}$  in Figure 2b and in faster convergence rates in Figure 2a. Because the majorizer design algorithm in this chapter can generate a majorizer with both circulant and diagonal components, it can capture the nonuniform weighting in  $\mathbf{H}$  better than  $\mathbf{M}_{\text{Circ}}$ . This results in further improvement over  $\mathbf{M}_{\text{Circ}}$ .

### B. X-ray CT reconstruction

Consider the following unconstrained X-ray CT reconstruction problem:

$$\hat{\mathbf{x}} = \underset{\mathbf{x}}{\operatorname{argmin}} \frac{1}{2} \|\mathbf{Ax} - \mathbf{y}\|_{\mathbf{W}}^2 + R(\mathbf{x}) \quad (40)$$

with X-ray CT system matrix  $\mathbf{A}$ , noisy measurements  $\mathbf{y}$ , diagonal matrix of positive statistical weights  $\mathbf{W}$  and edge-preserving regularizer  $R$  [23]. In this experiment, we assume the edge-preserving regularizer  $R$  is differentiable. The statistical weights  $\mathbf{W}$  contain patient-specific data that one can separate from the large CT system matrix with variable splitting:

$$\hat{\mathbf{x}} = \underset{\mathbf{x}}{\operatorname{argmin}} \frac{1}{2} \|\mathbf{u} - \mathbf{y}\|_{\mathbf{W}}^2 + R(\mathbf{x}) \quad \text{such that } \mathbf{u} = \mathbf{Ax}. \quad (41)$$

Applying the alternating directions method of multipliers (ADMM) to this constrained problem yields the following set of iterated updates [18], [20] with positive-definite penalty matrix  $\mathbf{\Gamma}$  and dual variable  $\boldsymbol{\eta}_u$ :

$$\mathbf{u}^{(n+1)} = (\mathbf{W} + \mathbf{\Gamma})^{-1} \left( \mathbf{Wy} + \mathbf{\Gamma}(\mathbf{Ax}^{(n)} + \boldsymbol{\eta}_u^{(n)}) \right) \quad (42)$$

$$\mathbf{x}^{(n+1)} = \underset{\mathbf{x}}{\operatorname{argmin}} \frac{1}{2} \|\mathbf{Ax} - \mathbf{u}^{(n+1)} + \boldsymbol{\eta}_u^{(n)}\|_{\mathbf{\Gamma}}^2 + R(\mathbf{x}) \quad (43)$$

$$\boldsymbol{\eta}_u^{(n+1)} = \boldsymbol{\eta}_u^{(n)} + \mathbf{Ax}^{(n+1)} - \mathbf{u}^{(n+1)}. \quad (44)$$

We can choose  $\mathbf{\Gamma}$  to make the  $\mathbf{u}$  update (42) easy, and the dual variable update (44) is trivial. For this experiment, we follow the guidance in [20] and set

$$\mathbf{\Gamma} = \operatorname{median}\{w_i\} \cdot \mathbf{I}. \quad (45)$$

The only challenging operation in this algorithm is the  $\mathbf{x}$  update (43) involving the computationally expensive CT system matrix  $\mathbf{A}$ .



Fig. 3: Initial image from filtered backprojection (3a) and the output of the ADMM algorithm with majorizer  $\mathbf{M}_{\text{Down}}$  after 64 iterations (3b).

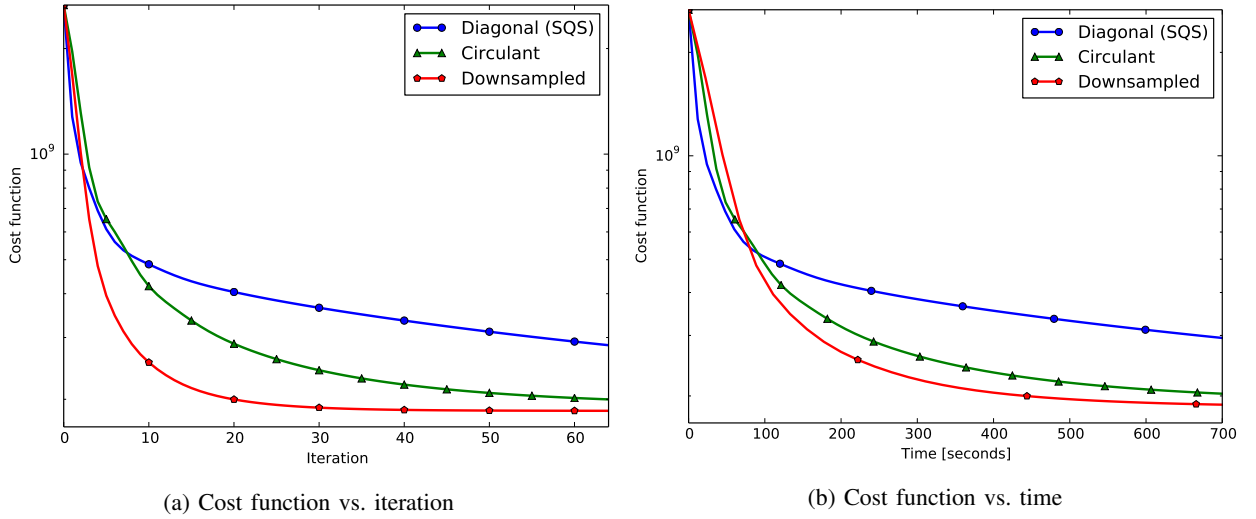


Fig. 4: Per-iteration (4a) and per-time (4b) cost function values for the ADMM algorithm using the three majorizers  $\mathbf{M}_{\text{SQS}}$ ,  $\mathbf{M}_{\text{Circ}}$  and  $\mathbf{M}_{\text{Down}}$ .

Let  $\mathbf{M} \succeq \mathbf{A}^\top \mathbf{\Gamma} \mathbf{A}$  be a majorizer for the quadratic term in Hessian of the  $\mathbf{x}$  update (43). Instead of solving (43) exactly, we majorize the quadratic term and descend the surrogate function

$$\mathbf{x}^{(n+1)} \approx \underset{\mathbf{x}}{\operatorname{argmin}} \frac{1}{2} \left\| \mathbf{x} - \mathbf{x}^{(n)} \right\|_{\mathbf{M}}^2 + \left( \mathbf{x} - \mathbf{x}^{(n)} \right)^\top \mathbf{A}^\top \mathbf{\Gamma} \left( \mathbf{A} \mathbf{x}^{(n)} - \mathbf{u}^{(n+1)} + \boldsymbol{\eta}_u^{(n)} \right) + \mathbf{R}(\mathbf{x}) \quad (46)$$

using five iterations of conjugate gradients.

We simulated a noisy 2D fan-beam scan of an XCAT [22] phantom with an 888-channel detector and 984 views, and then reconstructed images onto a  $512 \times 512$ -pixel grid. Figure 3a shows the initial image  $\mathbf{x}^{(0)}$  from filtered backprojection.

We ran the ADMM algorithm (42)-(44) with the following majorizers  $\mathbf{M}$  for the  $\mathbf{x}$  update:

- the diagonal majorizer  $\mathbf{M}_{\text{SQS}}$  (1);
- a circulant majorizer  $\mathbf{M}_{\text{Circ}}$  found by the proposed majorizer design algorithm with  $\mathbf{K} = \mathbf{U}_{\text{DFT}}$ ; and

- a majorizer using a “downsampled” version of the CT Gram matrix  $\mathbf{A}^T \mathbf{A}$ ,  $\mathbf{M}_{\text{Down}}$ . We set

$$\mathbf{K}_{\text{Down}} = \begin{bmatrix} \mathbf{A}_{\text{Down}} \\ \mathbf{I} \end{bmatrix}, \quad (47)$$

and used the proposed majorizer design algorithm, so  $\mathbf{M}_{\text{Down}}$  was a sum of a diagonal matrix and an approximation to the CT Gram matrix. For this experiment,  $\mathbf{A}_{\text{Down}}$  was a fan-beam CT system matrix that matched  $\mathbf{A}$  except it had 82 (instead of 984) views and 128 (instead of 888) channels. The downsampled  $\mathbf{A}_{\text{Down}}$  system had the same spatial coverage as the full system  $\mathbf{A}$  but lower computational cost.

We ran the majorizer design algorithm for 128 iterations for both  $\mathbf{M}_{\text{Circ}}$  and  $\mathbf{M}_{\text{Down}}$ , and used the looser  $\alpha = 3$  scaling to ensure majorization (see Section II-B).

All algorithms were run on a machine with a 12-core Intel Xeon processor, and multiplications with the system matrix  $\mathbf{A}$  were performed using multithreaded C code. Figure 3b shows the output of ADMM algorithm using  $\mathbf{M}_{\text{Down}}$  after 64 iterations. This is a preliminary experiment, and we do not yet have an essentially converged reference image to which to compare the tested algorithms, so we use the cost function at each iteration instead. Figures 4a and 4b show how quickly each algorithm descends the cost function (40) as functions of iteration and time, respectively.

Because the designed majorizers  $\mathbf{M}_{\text{Circ}}$  and  $\mathbf{M}_{\text{Down}}$  capture more of the structure of the Hessian  $\mathbf{H} = \mathbf{A}^T \mathbf{A}$ , they serve as both majorizers and preconditioners in the  $\mathbf{x}$  update (43). This allows the ADMM algorithm using these majorizers to converge more rapidly than when using the less-structured diagonal majorizer  $\mathbf{M}_{\text{SQS}}$ . Thanks to the FFT, the circulant majorizer  $\mathbf{M}_{\text{Circ}}$  is only marginally more computationally expensive than  $\mathbf{M}_{\text{Diag}}$ . On the other hand,  $\mathbf{M}_{\text{Down}}$  uses an approximation to the geometry of the original CT system matrix that makes it less computationally expensive than  $\mathbf{A}^T \mathbf{A}$ . This allows  $\mathbf{M}_{\text{Down}}$  to capture more of  $\mathbf{A}^T \mathbf{A}$ ’s structure than  $\mathbf{M}_{\text{Circ}}$ , leading to even faster convergence. While one could design a circulant majorizer for  $\mathbf{A}^T \mathbf{A}$  using its point spread function and power iteration, it is less clear how one would design a majorizer like  $\mathbf{M}_{\text{Down}}$  without an algorithm like the one proposed in this paper.

The ADMM-based reconstruction algorithms in this section may not converge quickly in absolute terms, especially compared to contemporary fast CT reconstruction algorithms [12]–[14], [18], but this experiment does show the benefits from using more sophisticated majorizers. Each of [12]–[14], [18] use diagonal SQS-like majorizers, and they may benefit from algorithmically designed majorizers.

#### IV. CONCLUSIONS AND FUTURE WORK

In this paper, we proposed a new way to design matrix majorizers. Our algorithm uses a duality-based approach to avoid relying on memory- and computation-intensive semidefinite programming (SPD) techniques. We proposed a simple steepest ascent algorithm to find a local maximum of the nonconcave dual problem, and we showed how to manipulate suboptimal solutions to guarantee a majorizer. In two preliminary experiments, we demonstrated the usefulness of the algorithmically designed majorizers. By capturing more of the structure of the majorized matrix, algorithmically designed majorizers with appropriately chosen structures can yield significant acceleration.

The experiments in this paper are preliminary, and future work will present comparisons with state-of-the-art image reconstruction algorithms. The majorizer structure in this paper can also be used to design so-called block-separable surrogates [9] that may be useful in distributed computing.

#### ACKNOWLEDGMENTS

The authors acknowledge helpful discussions with Dr. Sathish Ramani about majorizer design.

#### REFERENCES

- [1] H. Erdogan and J. A. Fessler. Ordered subsets algorithms for transmission tomography. *Phys. Med. Biol.*, 44(11):2835–51, November 1999.
- [2] S. Boyd and L. Vandenberghe. *Convex optimization*. Cambridge, UK, 2004.
- [3] T. F. Chan. An optimal circulant preconditioner for Toeplitz systems. *SIAM J. Sci. Stat. Comp.*, 9(4):766–71, July 1988.
- [4] E. Chouzenoux, J. Idier, and Said Moussaoui. A majorize-minimize strategy for subspace optimization applied to image restoration. *IEEE Trans. Im. Proc.*, 20(6):1517–28, June 2011.
- [5] N. H. Clinthorne, T. S. Pan, P. C. Chiao, W. L. Rogers, and J. A. Stamos. Preconditioning methods for improved convergence rates in iterative reconstructions. *IEEE Trans. Med. Imag.*, 12(1):78–83, March 1993.
- [6] J. de Leeuw and K. Lange. Sharp quadratic majorization in one dimension. *Comp. Stat. Data Anal.*, 53(7):2471–84, May 2009.
- [7] J. A. Fessler, N. H. Clinthorne, and W. L. Rogers. On complete data spaces for PET reconstruction algorithms. *IEEE Trans. Nuc. Sci.*, 40(4):1055–61, August 1993.
- [8] R. Fletcher. Semi-definite matrix constraints in optimization. *SIAM J. Cont. Opt.*, 23(4):493–, July 1985.
- [9] D. Kim and J. A. Fessler. Distributed block-separable ordered subsets for helical X-ray CT image reconstruction. In *Proc. Intl. Mtg. on Fully 3D Image Recon. in Rad. and Nuc. Med.*, pages 138–41, 2015.
- [10] D. Kim and J. A. Fessler. Optimized gradient methods for smooth convex minimization. In *Intl. Symp. Math. Prog.*, 2015. Submitted.
- [11] D. Kim, D. Pal, J.-B. Thibault, and J. A. Fessler. Accelerating ordered subsets image reconstruction for X-ray CT using spatially non-uniform optimization transfer. *IEEE Trans. Med. Imag.*, 32(11):1965–78, November 2013.
- [12] D. Kim, S. Ramani, and J. A. Fessler. Combining ordered subsets and momentum for accelerated X-ray CT image reconstruction. *IEEE Trans. Med. Imag.*, 34(1):167–78, January 2015.

- [13] M. G. McGaffin and J. A. Fessler. Alternating dual updates algorithm for X-ray CT reconstruction on the GPU. *IEEE Trans. Comp. Imag.*, 2015. To appear.
- [14] M. G. McGaffin and J. A. Fessler. Fast GPU-driven model-based X-ray CT image reconstruction via alternating dual updates. In *Proc. Intl. Mtg. on Fully 3D Image Recon. in Rad. and Nuc. Med.*, pages 312–5, 2015.
- [15] M. J. Muckley, D. C. Noll, and J. A. Fessler. Fast parallel MR image reconstruction via B1-based, adaptive restart, iterative soft thresholding algorithms (BARISTA). *IEEE Trans. Med. Imag.*, 34(2):578–88, February 2015.
- [16] Y. Nesterov. A method for unconstrained convex minimization problem with the rate of convergence  $O(1/k^2)$ . *Dokl. Akad. Nauk. USSR*, 269(3):543–7, 1983.
- [17] Y. Nesterov. Smooth minimization of non-smooth functions. *Mathematical Programming*, 103(1):127–52, May 2005.
- [18] H. Nien and J. A. Fessler. Fast X-ray CT image reconstruction using a linearized augmented Lagrangian method with ordered subsets. *IEEE Trans. Med. Imag.*, 34(2):388–99, February 2015.
- [19] Werner Oettli and Dirk Schlöger. Conjugate functions for convex and nonconvex duality. *Journal of Global Optimization*, 13(4):337–347, 1998.
- [20] S. Ramani and J. A. Fessler. A splitting-based iterative algorithm for accelerated statistical X-ray CT reconstruction. *IEEE Trans. Med. Imag.*, 31(3):677–88, March 2012.
- [21] S. Ramani and J. A. Fessler. Accelerated nonCartesian SENSE reconstruction using a majorize-minimize algorithm combining variable-splitting. In *Proc. IEEE Intl. Symp. Biomed. Imag.*, pages 704–7, 2013.
- [22] W. P. Segars, M. Mahesh, T. J. Beck, E. C. Frey, and B. M. W. Tsui. Realistic CT simulation using the 4D XCAT phantom. *Med. Phys.*, 35(8):3800–8, August 2008.
- [23] J-B. Thibault, K. Sauer, C. Bouman, and J. Hsieh. A three-dimensional statistical approach to improved image quality for multi-slice helical CT. *Med. Phys.*, 34(11):4526–44, November 2007.

## APPENDIX A STRONG DUALITY

Let  $\mathbf{H} \in \mathbb{C}^{N \times N} \succ \mathbf{0}$  be a given positive semidefinite matrix,  $\mathbf{K} \in \mathbb{C}^{K \times N}$ ,  $K \geq N$  have full column rank and define  $\Omega$  to be

$$\Omega = \{\mathbf{d} : \mathbf{K}^H \mathbf{D} \mathbf{K} \succeq \mathbf{H}\}. \quad (48)$$

Consider the function

$$S(\mathbf{d}, \mathbf{z}) = \frac{1}{2} \|\mathbf{d}\|_{\mathbf{W}}^2 - \mathbf{d}^T |\mathbf{K} \mathbf{z}|^2 + \mathbf{z}^H \mathbf{H} \mathbf{z}. \quad (49)$$

The primal function is

$$J(\mathbf{d}) = \sup_{\mathbf{z} \in \mathbb{C}^N} S(\mathbf{d}, \mathbf{z}) \quad (50)$$

$$= \frac{1}{2} \|\mathbf{d}\|_{\mathbf{W}}^2 + \iota_{\Omega}(\mathbf{d}). \quad (51)$$

and the dual function is

$$L(\mathbf{z}) = \inf_{\mathbf{d} \in \mathbb{R}^K} S(\mathbf{d}, \mathbf{z}) \quad (52)$$

$$= -\frac{1}{2} \left\| |\mathbf{K} \mathbf{z}|^2 \right\|_{\mathbf{W}^{-1}}^2 + \mathbf{z}^H \mathbf{H} \mathbf{z}. \quad (53)$$

In this section we show the minimum of the primal function is equal to the maximum of the dual function:

$$p = \min_{\mathbf{d} \in \mathbb{R}^K} J(\mathbf{d}) = \sup_{\mathbf{z} \in \mathbb{C}^N} L(\mathbf{z}) = d. \quad (54)$$

Because  $J$  is a strongly convex function and  $\Omega$  is a convex set, there exists a unique minimizer of  $J$  over  $\Omega$ . Let  $\hat{\mathbf{d}}$  be this minimizer:

$$\hat{\mathbf{d}} = \operatorname{argmin}_{\mathbf{d} \in \Omega} J(\mathbf{d}). \quad (55)$$

Because  $\mathbf{H} \succ \mathbf{0}$  the unconstrained minimizer of  $\frac{1}{2} \|\mathbf{d}\|_{\mathbf{W}}^2$ ,  $\mathbf{d}_{\text{unconstrained}} = \mathbf{0}$ , does not lie in  $\Omega$ . Therefore,  $\hat{\mathbf{d}}$  is on the boundary of  $\Omega$  and  $-\nabla J(\hat{\mathbf{d}}) = \mathbf{W} \hat{\mathbf{d}}$  is normal to  $\Omega$ .

We can characterize the feasible set  $\Omega$  as an intersection of half-spaces:

$$\Omega = \bigcap_{\mathbf{z}} \{\mathbf{d} : \mathbf{z}^H (\mathbf{K}^H \mathbf{D} \mathbf{K} - \mathbf{H}) \mathbf{z} \geq 0\} \quad (56)$$

$$= \bigcap_{\mathbf{z}} \{\mathbf{d} : \mathbf{d}^T |\mathbf{K} \mathbf{z}|^2 \geq \mathbf{z}^H \mathbf{H} \mathbf{z}\}. \quad (57)$$

Because  $-\nabla J(\hat{\mathbf{d}}) = \mathbf{W} \hat{\mathbf{d}}$  is normal to  $\Omega$  and on the boundary of  $\Omega$ , there exists an  $\hat{\mathbf{z}}$  for which one of the above inequalities holds with equality. That is,

$$-\nabla J(\hat{\mathbf{d}}) = \mathbf{W} \hat{\mathbf{d}} = \alpha |\mathbf{K} \hat{\mathbf{z}}|^2 \quad (58)$$



and

$$\widehat{\mathbf{z}}^H \mathbf{H} \widehat{\mathbf{z}} = \widehat{\mathbf{d}}^T |\mathbf{K} \widehat{\mathbf{z}}|^2 = \alpha \left( |\mathbf{K} \widehat{\mathbf{z}}|^2 \right)^T \mathbf{W}^{-1} |\mathbf{K} \widehat{\mathbf{z}}|^2 = \alpha \left\| |\mathbf{K} \widehat{\mathbf{z}}|^2 \right\|_{\mathbf{W}^{-1}}^2. \quad (59)$$

We use (58) to find the minimum of the primal function:

$$J(\widehat{\mathbf{d}}) = \frac{1}{2} \left\| \widehat{\mathbf{d}} \right\|_{\mathbf{W}}^2 \quad (60)$$

$$= \frac{1}{2} \left\| \alpha \mathbf{W}^{-1} |\mathbf{K} \widehat{\mathbf{z}}|^2 \right\|_{\mathbf{W}}^2 \quad (61)$$

$$= \frac{\alpha^2}{2} \left\| |\mathbf{K} \widehat{\mathbf{z}}|^2 \right\|_{\mathbf{W}^{-1}}^2 \quad (62)$$

$$= p. \quad (63)$$

It is widely known that  $p \geq d$ . Therefore, to show  $p = d$  it suffices to show that  $L(\mathbf{z}) = p$  for some  $\mathbf{z}$ . We try  $L(\beta \widehat{\mathbf{z}})$ , with  $\beta^2 = \alpha$ :

$$L(\beta \widehat{\mathbf{z}}) = -\frac{1}{2} \left\| \beta |\mathbf{K} \widehat{\mathbf{z}}|^2 \right\|_{\mathbf{W}^{-1}}^2 + \beta^2 \widehat{\mathbf{z}}^T \mathbf{H} \widehat{\mathbf{z}} \quad (64)$$

$$= -\frac{\beta^4}{2} \left\| |\mathbf{K} \widehat{\mathbf{z}}|^2 \right\|_{\mathbf{W}^{-1}}^2 + \beta^2 \widehat{\mathbf{z}}^T \mathbf{H} \widehat{\mathbf{z}} \quad (65)$$

via (59),

$$= -\frac{\beta^4}{2} \left\| |\mathbf{K} \widehat{\mathbf{z}}|^2 \right\|_{\mathbf{W}^{-1}}^2 + \beta^2 \alpha \left\| |\mathbf{K} \widehat{\mathbf{z}}|^2 \right\|_{\mathbf{W}^{-1}}^2 \quad (66)$$

$$= \frac{\alpha^2}{2} \left\| |\mathbf{K} \widehat{\mathbf{z}}|^2 \right\|_{\mathbf{W}^{-1}}^2 \quad (67)$$

$$= p, \quad (68)$$

completing the proof.

## APPENDIX B

### EQUIVALENCE OF MAJORIZERS FROM PRIMAL AND DUAL PROBLEMS

In this paper, instead of solving the primal problem

$$\widehat{\mathbf{D}} = \underset{\mathbf{d} \in \mathbb{R}^K}{\operatorname{argmin}} \frac{1}{2} \left\| \mathbf{d} \right\|_{\mathbf{W}}^2 + \iota_{\Omega}(\mathbf{d}) \quad (69)$$

$$= \underset{\mathbf{d} \in \mathbb{R}^K}{\operatorname{argmin}} \sup_{\mathbf{z} \in \mathbb{C}^N} \frac{1}{2} \left\| \mathbf{d} \right\|_{\mathbf{W}}^2 + \mathbf{z}^H \mathbf{H} \mathbf{z} - \mathbf{d}^T |\mathbf{K} \mathbf{z}|^2 \quad (70)$$

$$= \underset{\mathbf{d} \in \mathbb{R}^K}{\operatorname{argmin}} \sup_{\mathbf{z} \in \mathbb{C}^N} S(\mathbf{d}, \mathbf{z}), \quad (71)$$

we reverse the order of the minimization and maximization and solve the dual problem

$$\widehat{\mathbf{z}} = \underset{\mathbf{z} \in \mathbb{C}^N}{\operatorname{argmax}} \inf_{\mathbf{d} \in \mathbb{R}^K} S(\mathbf{d}, \mathbf{z}). \quad (72)$$

In this section, we prove that the primal solution

$$\widehat{\mathbf{D}}_p = \underset{\mathbf{d} \in \mathbb{R}^K}{\operatorname{argmin}} \sup_{\mathbf{z} \in \mathbb{C}^N} S(\mathbf{d}, \mathbf{z}) \quad (73)$$

and the solution induced by solving the dual problem

$$\widehat{\mathbf{D}}_d = \underset{\mathbf{d} \in \mathbb{R}^K}{\operatorname{argmin}} S(\mathbf{d}, \widehat{\mathbf{z}}), \quad (74)$$

where  $\widehat{\mathbf{z}}$  solves the dual problem (72), are equal.

Let  $d$  be the maximum value attained by the dual function at  $\widehat{\mathbf{z}}$  and  $p$  be the minimum value attained by the primal function at  $\widehat{\mathbf{d}}$ :

$$d = \sup_{\mathbf{z} \in \mathbb{C}^N} \inf_{\mathbf{d} \in \mathbb{R}^K} S(\mathbf{d}, \mathbf{z}), \quad (75)$$

$$p = \inf_{\mathbf{d} \in \mathbb{R}^K} \sup_{\mathbf{z} \in \mathbb{C}^N} S(\mathbf{d}, \mathbf{z}). \quad (76)$$

We proceed by contradiction. Assume that  $\widehat{\mathbf{D}}_p \neq \widehat{\mathbf{D}}_d$ . Since  $S(\mathbf{d}, \mathbf{z})$  is a strongly convex function of  $\mathbf{d}$

$$d = \sup_{\mathbf{z} \in \mathbb{C}^N} \inf_{\mathbf{d} \in \mathbb{R}^K} S(\mathbf{d}, \mathbf{z}) \quad (77)$$

$$= S(\mathbf{d}_d, \widehat{\mathbf{z}}) \quad (78)$$

$$< S(\mathbf{d}_p, \widehat{\mathbf{z}}) \quad (79)$$

$$\leq S \sup_{\mathbf{z} \in \mathbb{C}^N} (\mathbf{d}_p, \mathbf{z}) \quad (80)$$

$$= p. \quad (81)$$

That is,  $p \neq d$ . This contradicts the strong duality result in Section A, and we conclude that  $\widehat{\mathbf{D}} = \mathbf{D}_p = \mathbf{D}_d$ . Now we can write the primal solution  $\widehat{\mathbf{D}}$  in terms of dual solution  $\widehat{\mathbf{z}}$ :

$$\widehat{\mathbf{D}} = \underset{\mathbf{d} \in \mathbb{R}^K}{\operatorname{argmin}} S(\mathbf{d}, \widehat{\mathbf{z}}) \quad (82)$$

$$= \underset{\mathbf{d} \in \mathbb{R}^K}{\operatorname{argmin}} \frac{1}{2} \|\mathbf{d}\|_{\mathbf{W}}^2 - \mathbf{d}^\top |\mathbf{K}\mathbf{d}|^2 + \mathbf{z}^\mathbf{H} \mathbf{H} \mathbf{z} \quad (83)$$

$$= \mathbf{W}^{-1} |\mathbf{K}\mathbf{d}|^2. \quad (84)$$

#### APPENDIX C SCALING FOR MAJORIZATION

Let  $\widetilde{\mathbf{z}}$  be a local maximum of the nonconcave dual function  $L(\mathbf{z})$  found by an iterative gradient-based method. Because  $\widetilde{\mathbf{z}}$  is an attractor of the maximization procedure and  $L$  is smooth,  $L$  is concave at  $\widetilde{\mathbf{z}}$ . That is, the Hessian of  $L$  at  $\widetilde{\mathbf{z}}$  is nonpositive definite:

$$\nabla^2 L(\widetilde{\mathbf{z}}) = -6\mathbf{K}^\mathbf{H} \mathbf{W}^{-1} \operatorname{diag} \left\{ \left[ |\mathbf{K}\widetilde{\mathbf{z}}|^2 \right]_i \right\} \mathbf{K} + 2\mathbf{H} \preceq \mathbf{0}. \quad (85)$$

Rearranging,

$$3\mathbf{K}^\mathbf{H} \mathbf{W}^{-1} \operatorname{diag} \left\{ \left[ |\mathbf{K}\widetilde{\mathbf{z}}|^2 \right]_i \right\} \mathbf{K} \succeq \mathbf{H}. \quad (86)$$

Even though we do not find the global maximum of  $L$  using the steepest ascent procedure in Section II-A, simply scaling the majorizer produced by a local maximum by a factor of 3 produces a majorizer for  $\mathbf{H}$ .